

Neutron Star Properties from Low-Mass X-ray binary (LMXB)

Chang-Hwan Lee / Pusan National University

focused on Astronomy & Astrophysics 650, A139 (2021)

in collaboration with

Myungkuk Kim, Young-Min Kim, Kyujin Kwak (UNIST)

Contributions to QCS

- QCS2014: *Supercritical Accretion in the Evolution of Neutron Star Binaries and its Implications*
- QCS2017: *Strangeness in Neutron Star Cooling*
- QCS2019: *Chair of Organizing Committee*
- QCS2023: *Neutron Star Properties from Low-Mass X-ray Binary*

Astro-Hadron Physics *my main interests in Neutron Star related problems*

Hadron Physics

Astrophysics

Kaon Condensation in Dense Stellar Matter
(with **D.P.Min**, **M.Rho** & **G.E.Brown**)

1990s

NS Binary as a source of GW
(with **G.E.Brown**@Stony Brook)

2003

Korean Gravitational Wave Group

Science-Business-Belt Project
initiated by **D.P. Min**

2006

Nuclear physics + Astrophysics +
Mathematics + Artificial Intelligence

RAON project was approved

2009

KGWG joined LIGO Scientific Collab.

Transport Studies

DJBUU (new transport code)
BUD²-McGill Collaboration

2017

GW from NS-NS mergers
(Multi-messenger Astrophysics)
Tidal deformability of NS

First Beam of RAON

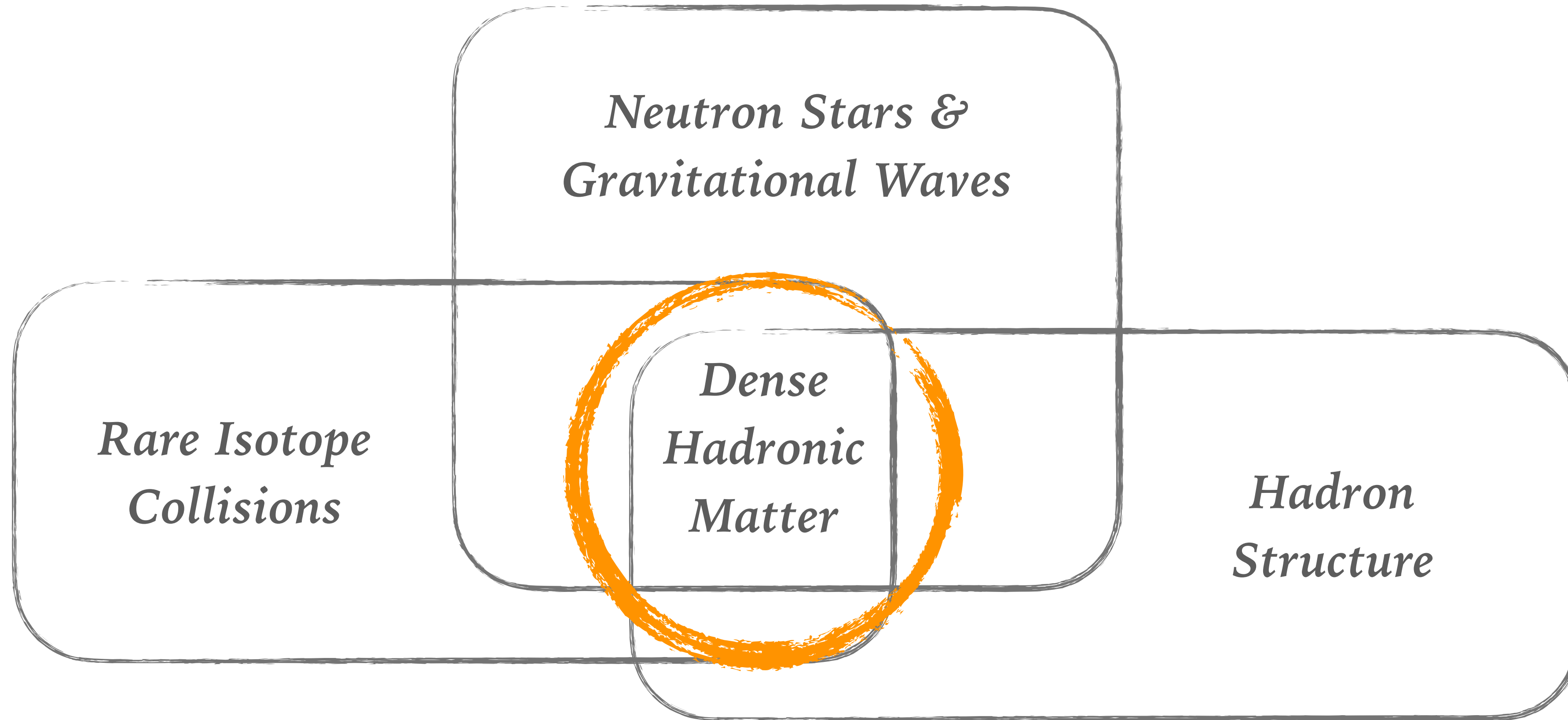
2022.10.07

2022

2023

for Astro-Hadron Physics

Astro-Hadron Physics Group@PNU



Dense Nuclear & Stellar Matter Studies

for **RAON** New Rare Isotope Accelerator & **MMA** Multi-Messenger Astrophysics



BUD² Collaboration

Busan (CHL, H.S. CHO,)

Ulsan (K. KWAK, Y.-M. KIM, M. KIM,)

Daegu (Chang Ho HYUN)

Daejeon (**Youngman KIM**,)

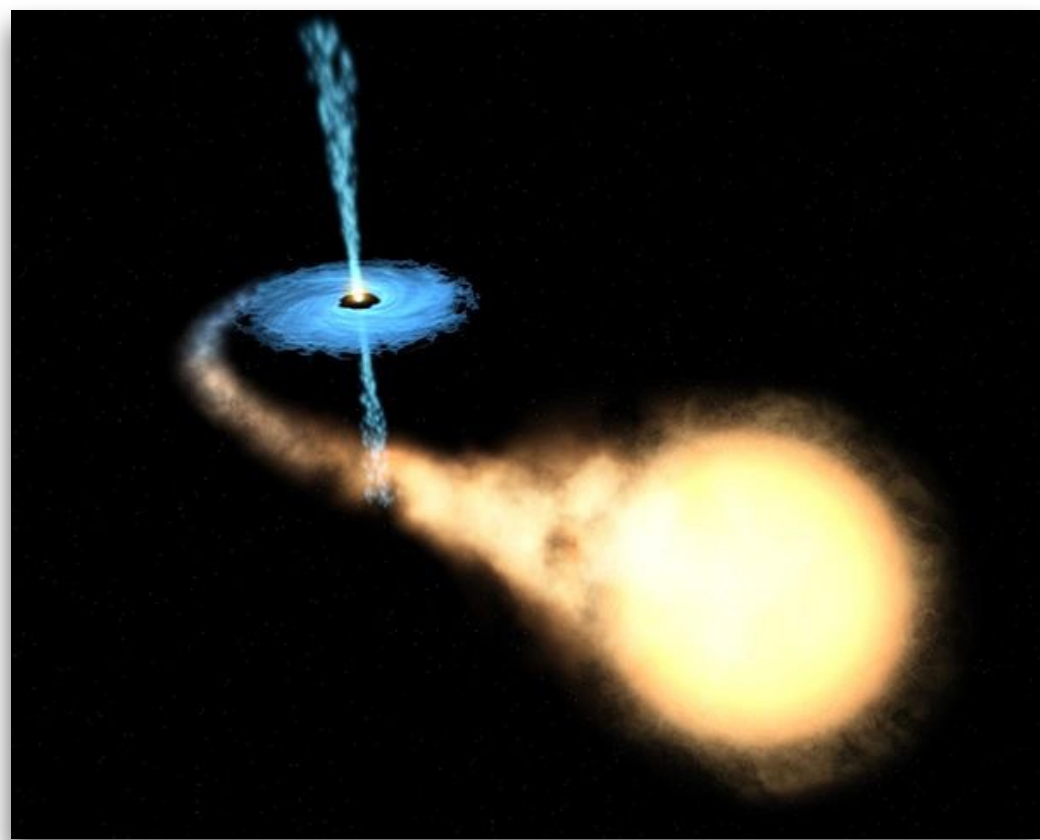
Montreal (Sangyong JEON, McGill)

Contents

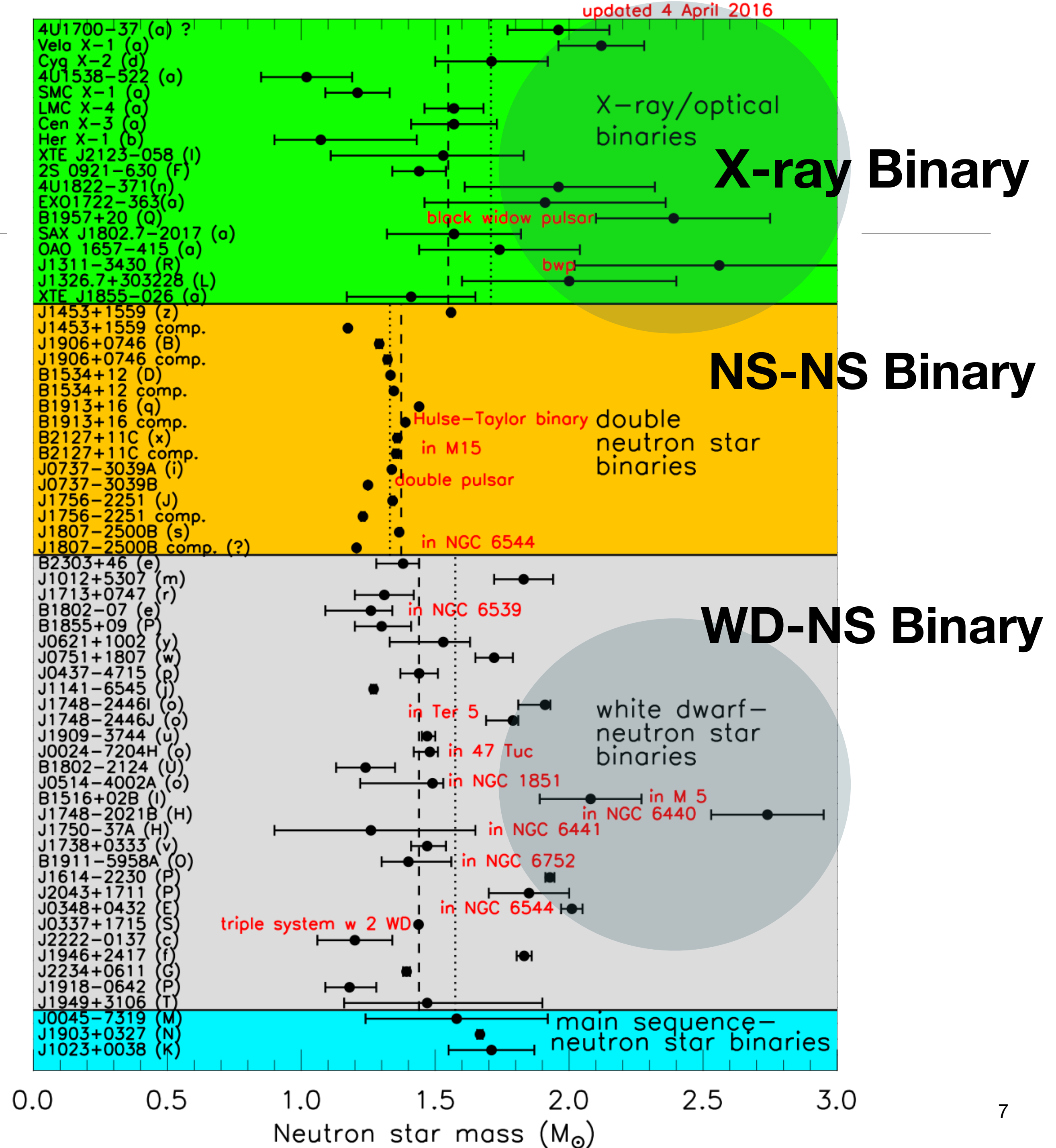
- Introduction & Motivation
- Mass & Radius of NS from Low-Mass X-ray binary (LMXB)
 - Monte Carlo sampling
 - Bayesian analysis
- Discussion

By EM observations before GW

- High-mass neutron stars in X-ray binaries have been reported
- But, they are not considered as evidences of the existence of high-mass NS due to large uncertainties

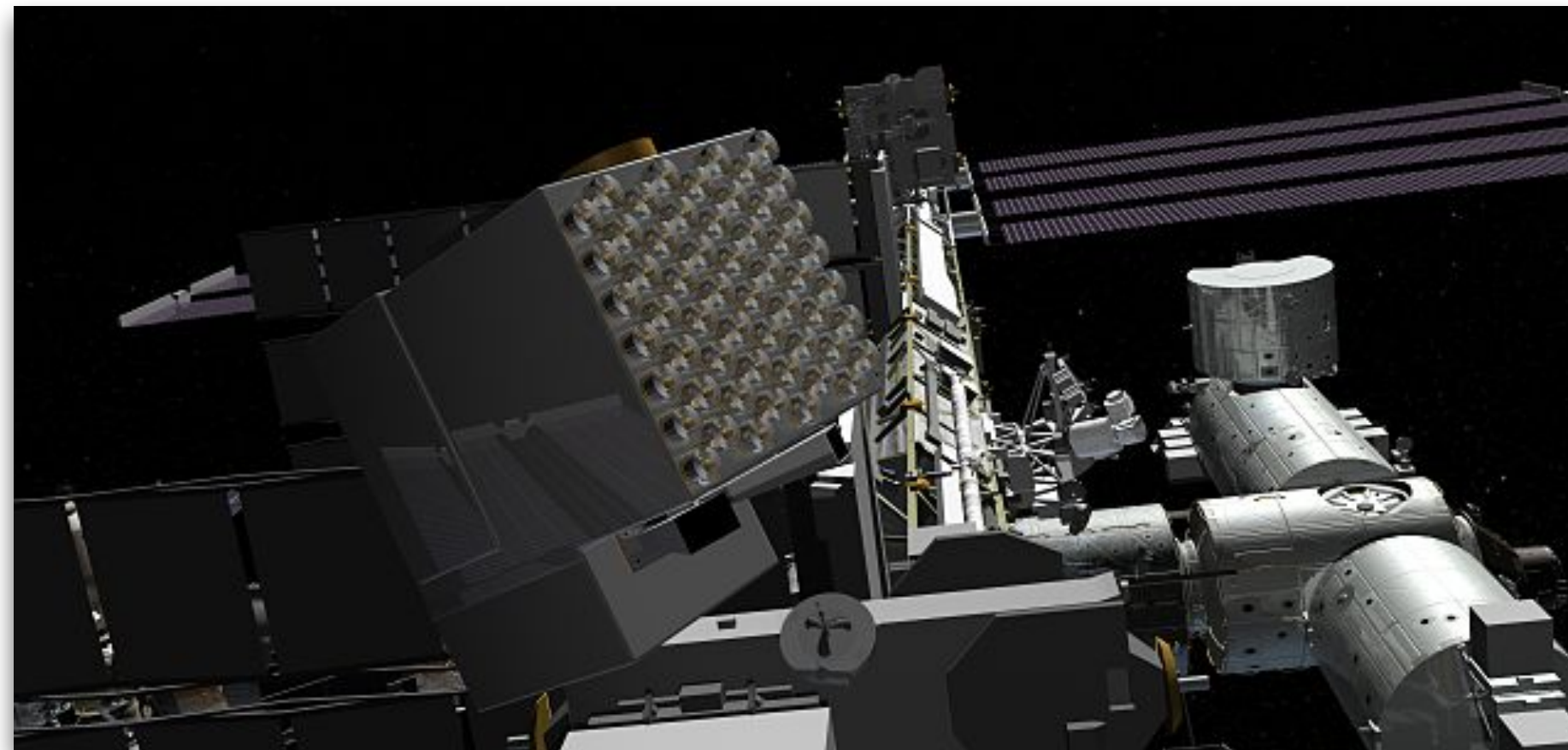
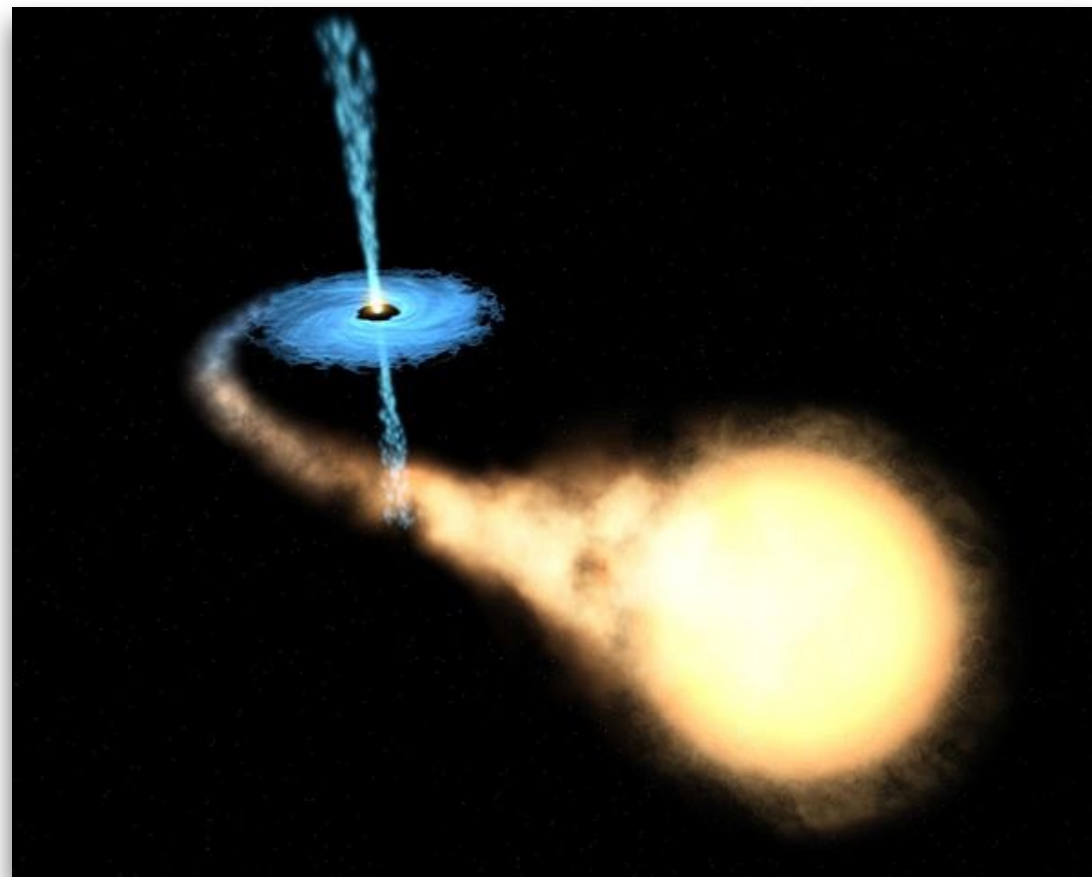


J. Lattimer



NICER Neutron star Interior Composition Explorer

- **launch:** June 2017, SpaceX
- **platform:** ISS ELC (ExPRESS Logistics Carrier)
- **instrument:** **X-ray (0.2-12 keV)**
- **objective**
 - **structure:** neutron star radii to 5%, cooling timescales
 - **dynamics:** stability of pulsars as clocks, properties of outbursts, oscillations, and precession
 - **energetics:** intrinsic radiation patterns, spectra, and luminosities

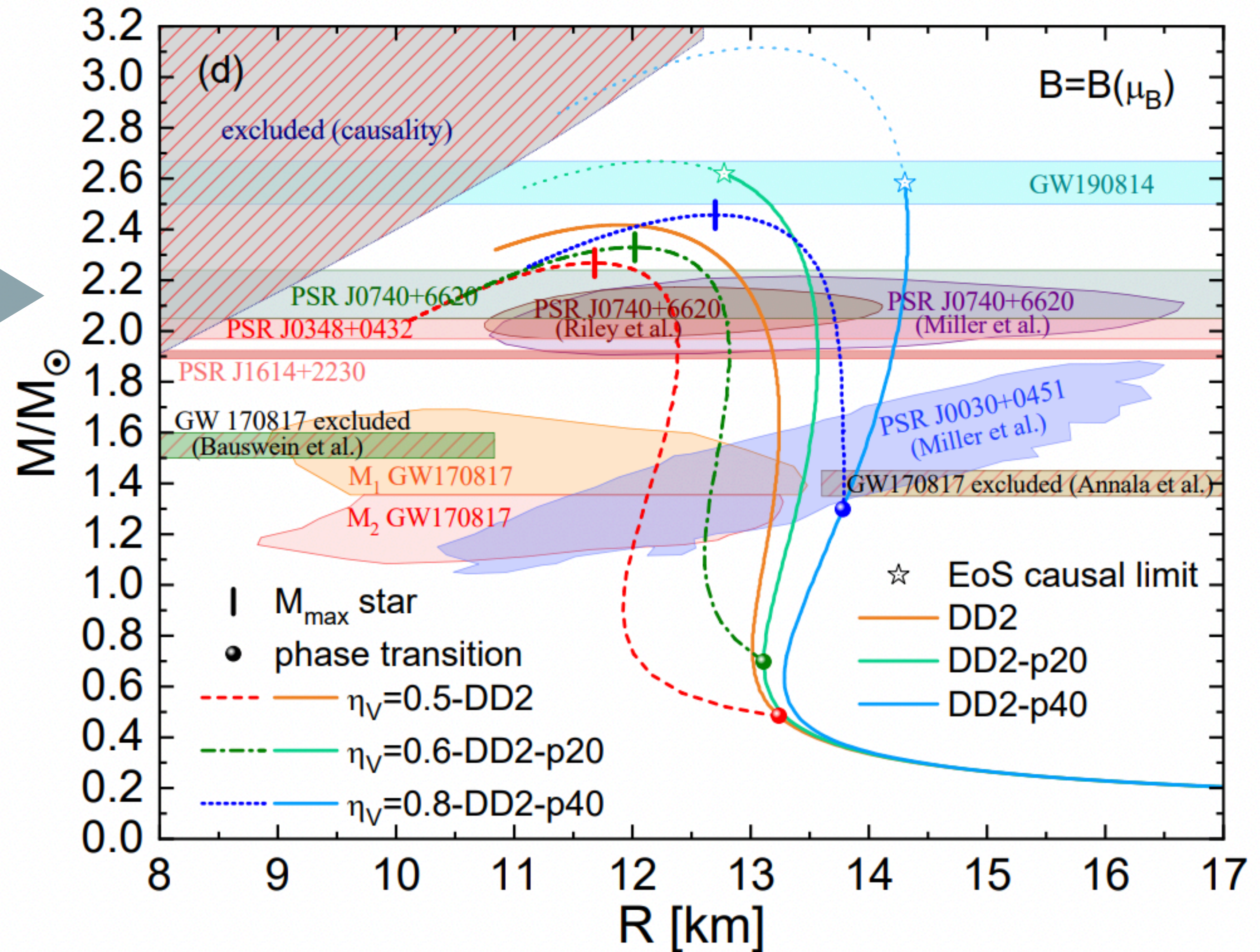


High-mass NS by NICER (X-ray : 0.2-12 keV)

WD-NS Binary
(radio/Shapiro delay) →

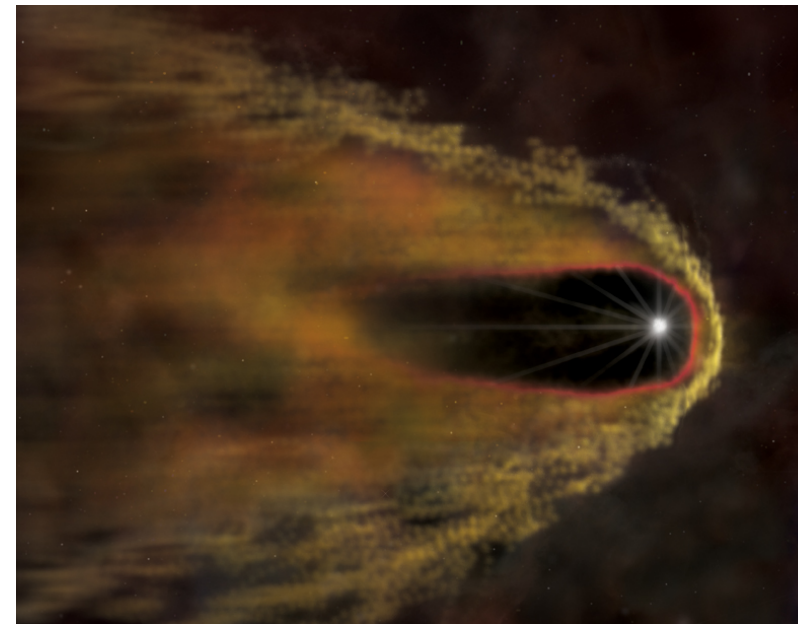
arXiv:2201.00477

Contrera, Blaschke,
Carlomagno, Grunfeld,
Liebbing

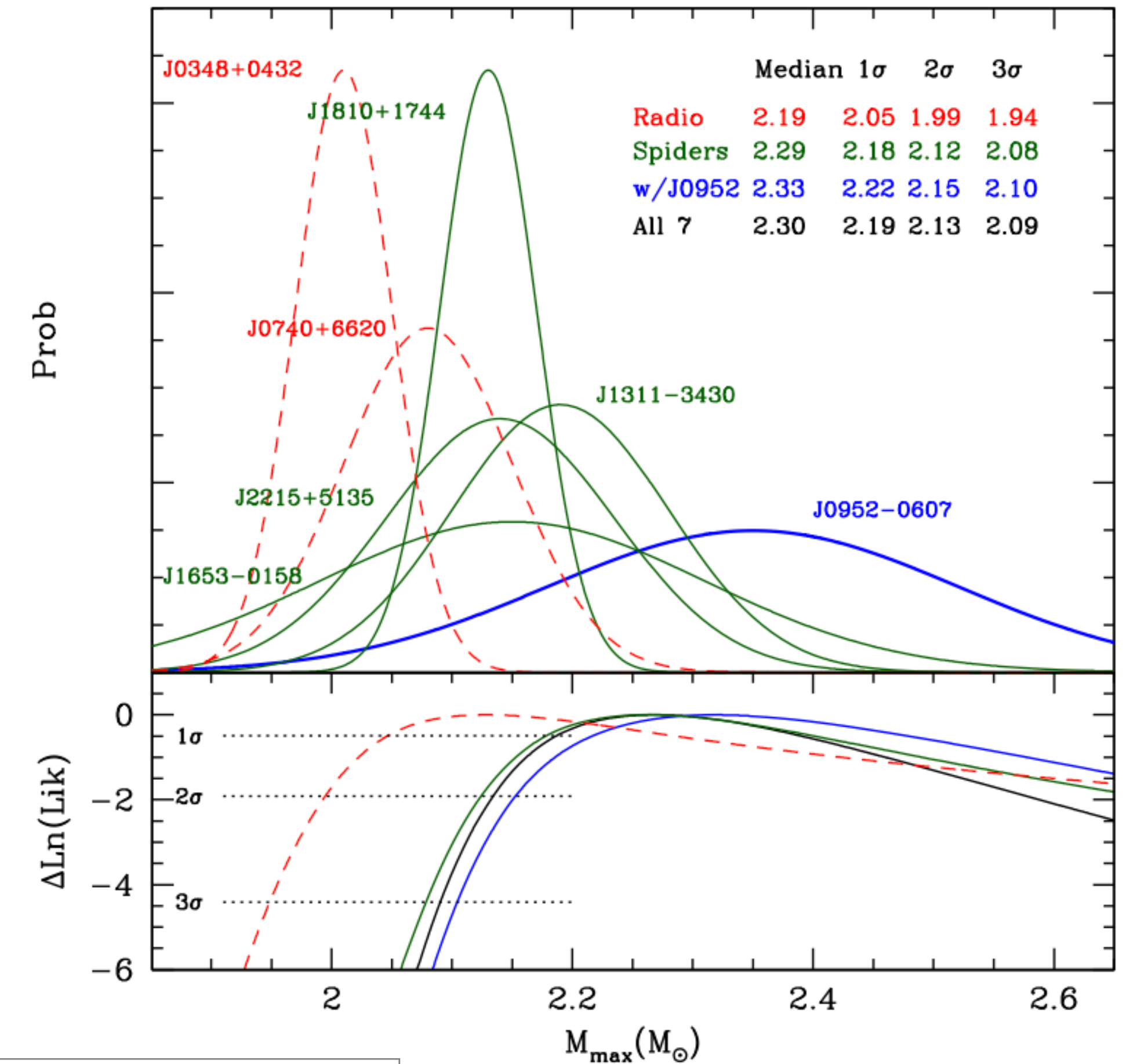


Black Widow Pulsar

Companion is destroyed by the strong powerful outflows, or winds, of high-energy particles caused by the neutron star



$$M_{\text{NS}} = 2.35 \pm 0.17 M_{\odot}$$



THE ASTROPHYSICAL JOURNAL LETTERS, 934:L17 (6pp), 2022 August 1

© 2022. The Author(s). Published by the American Astronomical Society.

<https://doi.org/10.3847/2041-8213/ac8007>

OPEN ACCESS



CrossMark

PSR J0952–0607: The Fastest and Heaviest Known Galactic Neutron Star

Roger W. Romani¹ , D. Kandel¹ , Alexei V. Filippenko² , Thomas G. Brink² , and WeiKang Zheng² 

GW 170817 (**d=40 Mpc**)

GRB 170817A by Fermi-GBM

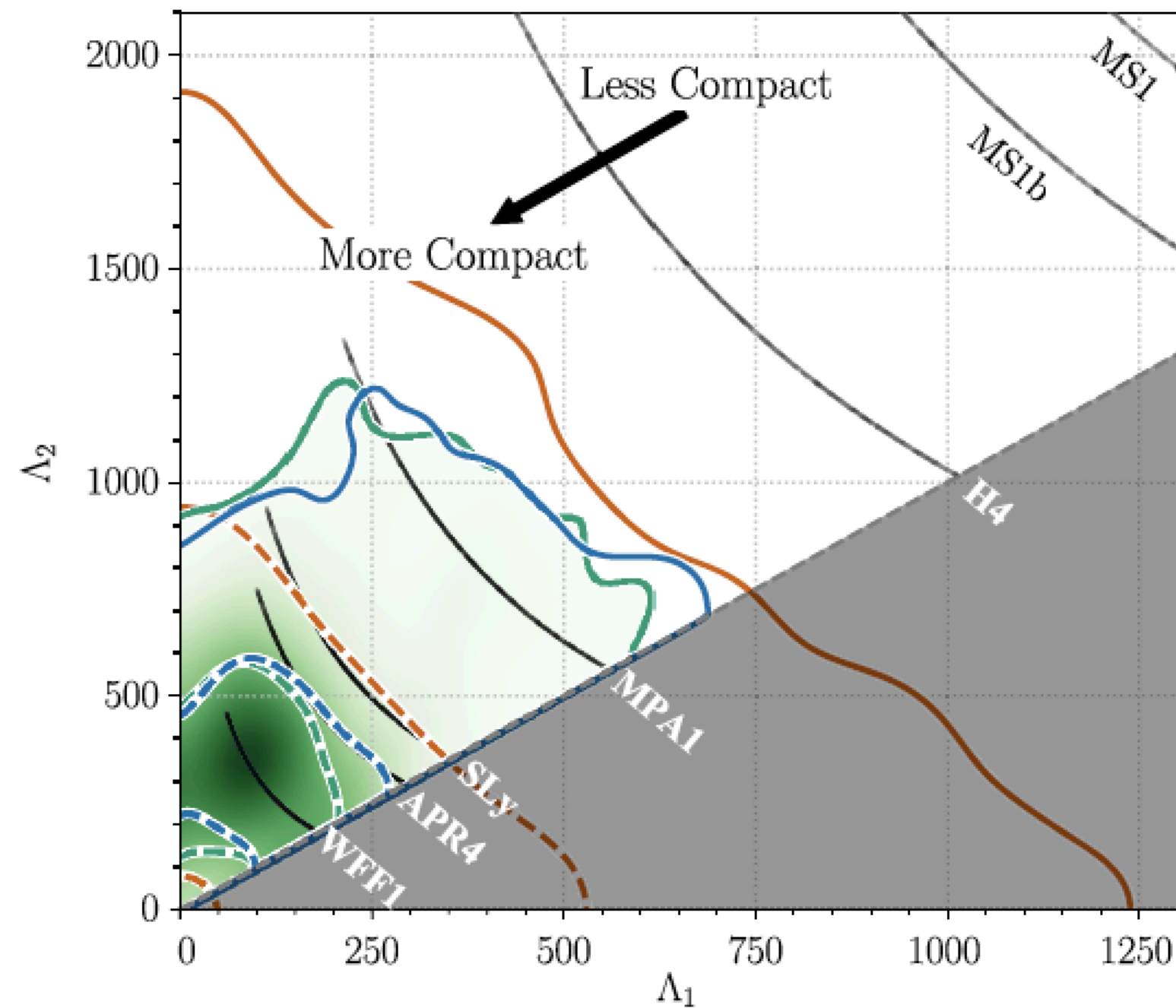
Kilonova/X-ray/Optical Afterglows

A new constraints by GW observations

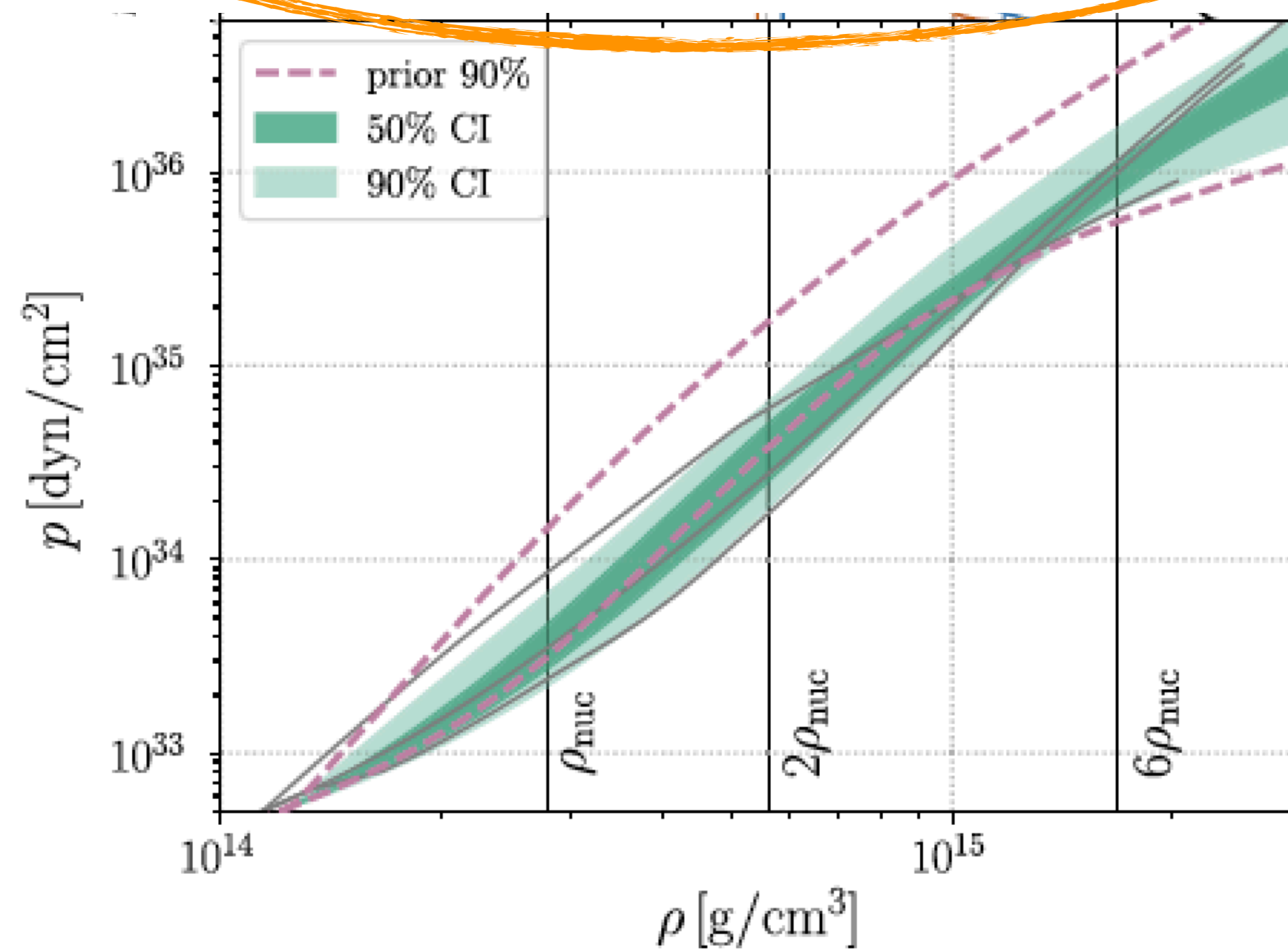
$$\Lambda_{1.4M_{\odot}} = 190^{+390}_{-120}$$

$$P_{2\rho_{\text{nuc}}} = 3.5^{+2.7}_{-1.7} \times 10^{34} \text{ dyne/cm}^2$$

$$P_{6\rho_{\text{nuc}}} = 9.0^{+7.9}_{-2.6} \times 10^{34} \text{ dyne/cm}^2$$



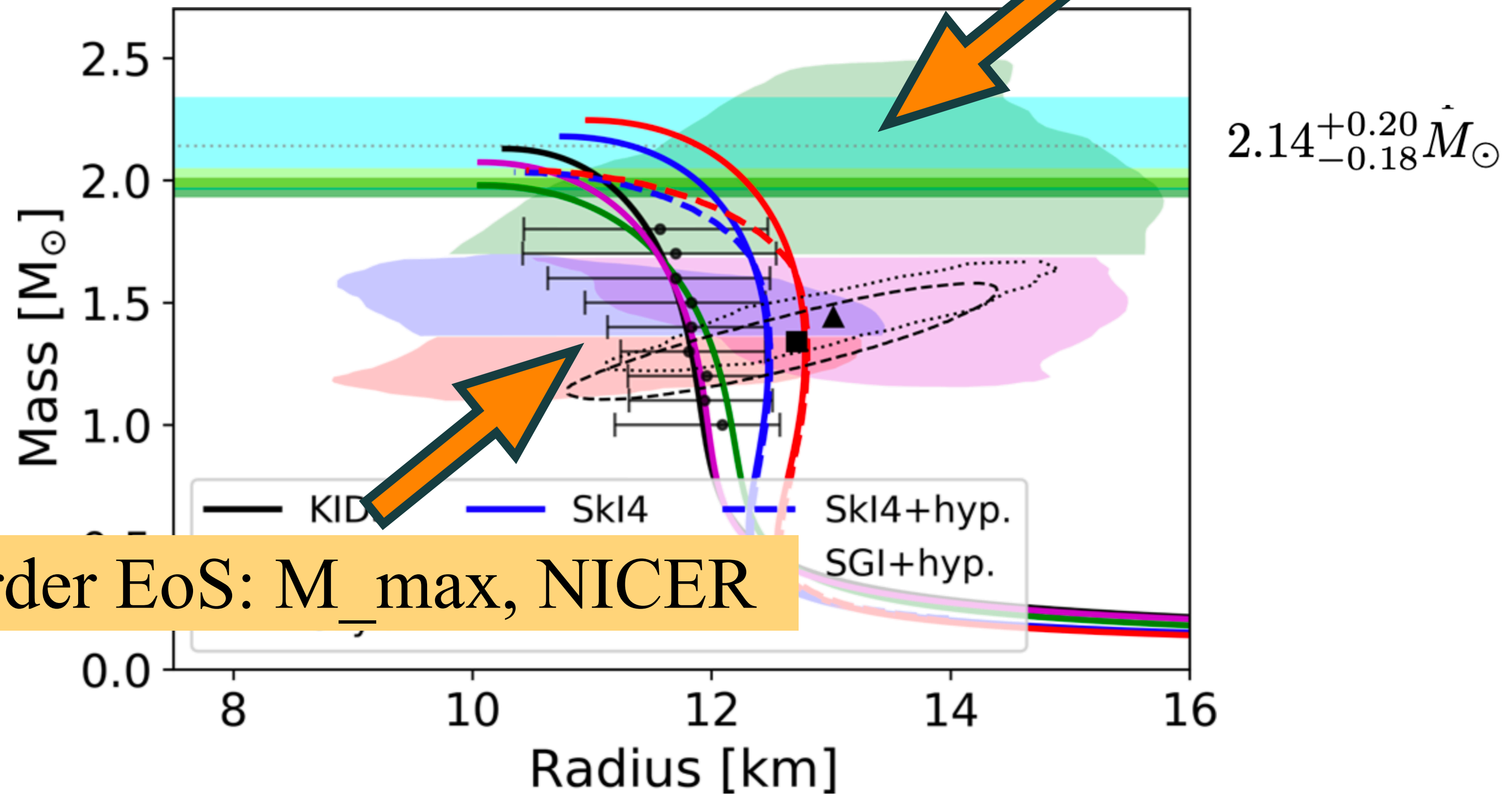
LSC and Virgo, PRL 121, 161101 (2018)



$$\rho_{\text{nuc}} = 2.8 \times 10^{14} \text{ g/cm}^3$$

Constraints on Equation of State

prefer soft EoS: GW170817, strangeness



prefer harder EoS: M_{max} , NICER

$2.6M_{\odot}$ **Black Hole or Neutron Star or Quark Star ?**

- **Light Black Hole**

- *e.g., Yang et al., ApJL 901, L34 (2020)*
- Tidal deformability of GW170817 **prefers soft EOS**
- 2.6 solar mass NS is **inconsistent with soft EOS** (requires hard EOS)
- Light BH may be formed **by accretion** (not from direct collapse of giant stars)

- **Strange Quark Star**

- *e.g., Bombaci et al., PRL 126, 162702 (2021)*
Drago & Pagliara, PRD 102, 063003 (2020)
- Two track scenario
- NS and QS may coexist

-

Low-Mass X-ray Binaries

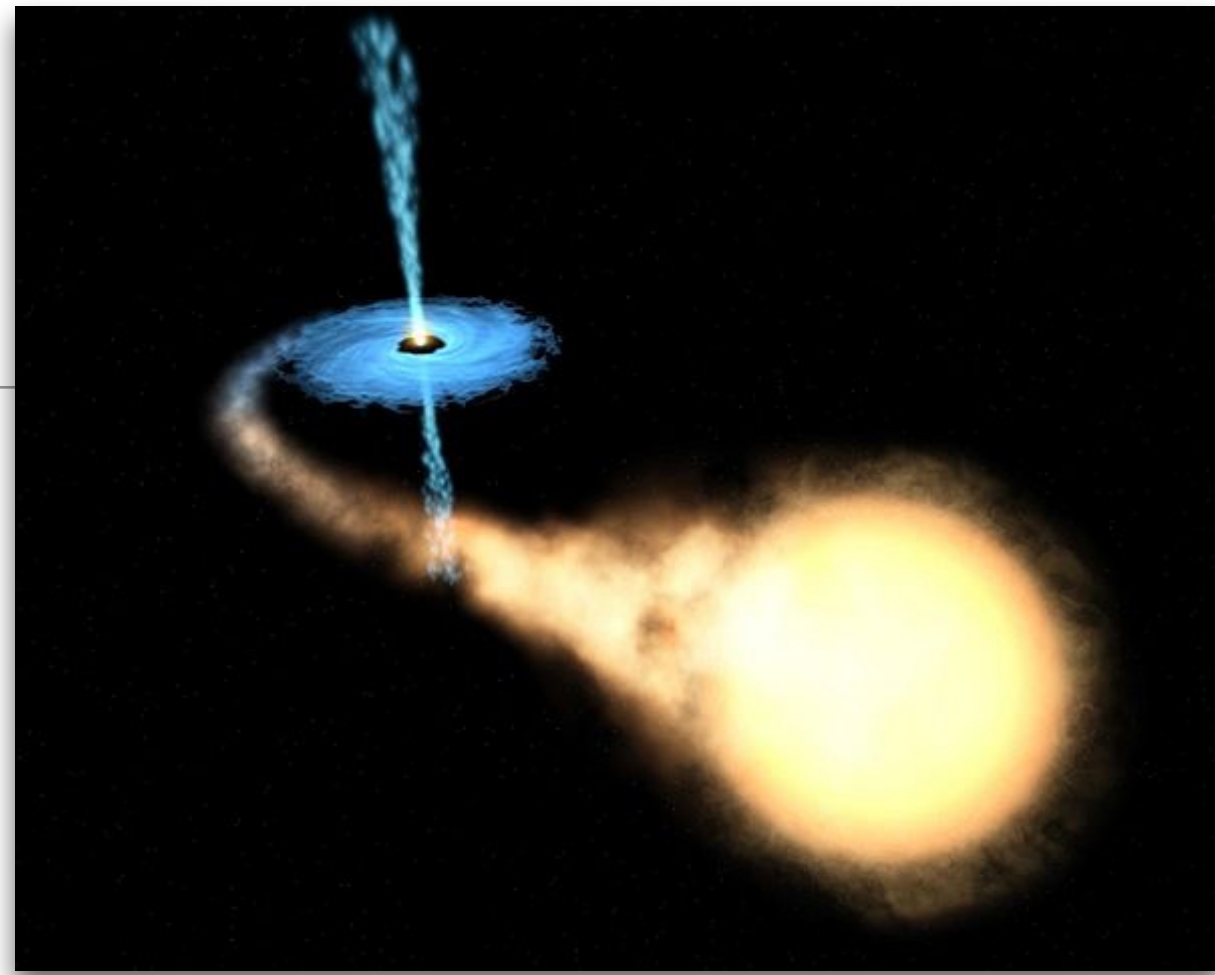
With Myungkuk Kim, Young-Min Kim, Kyujin Kwak

A&A 650, A139 (2021)
<https://doi.org/10.1051/0004-6361/202038126>
© ESO 2021

**Astronomy
&
Astrophysics**

Measuring the masses and radii of neutron stars in low-mass X-ray binaries: Effects of the atmospheric composition and touchdown radius

Myungkuk Kim¹, Young-Min Kim¹, Kwang Hyun Sung¹, Chang-Hwan Lee², and Kyujin Kwak¹



Low-Mass X-ray binary (low-mass companion)

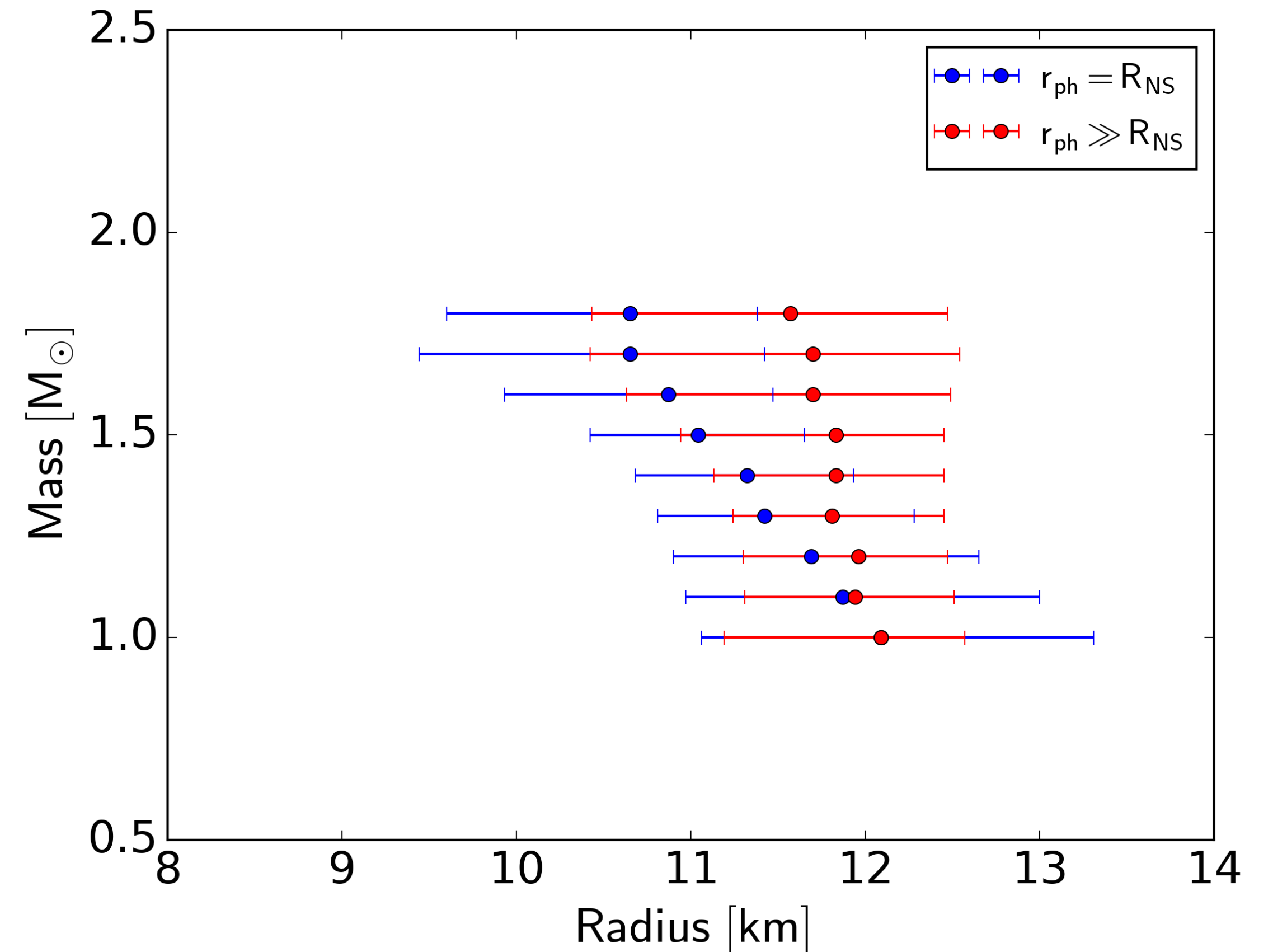
Table 9

Most Probable Values for Masses and Radii for Neutron Stars Constrained to Lie on One Mass Versus Radius Curve

Object	$M (M_{\odot})$	R (km)	$M (M_{\odot})$	R (km)
	$r_{\text{ph}} = R$		$r_{\text{ph}} \gg R$	
4U 1608–522	$1.52^{+0.22}_{-0.18}$	$11.04^{+0.53}_{-1.50}$	$1.64^{+0.34}_{-0.41}$	$11.82^{+0.42}_{-0.89}$
EXO 1745–248	$1.55^{+0.12}_{-0.36}$	$10.91^{+0.86}_{-0.65}$	$1.34^{+0.450}_{-0.28}$	$11.82^{+0.47}_{-0.72}$
4U 1820–30	$1.57^{+0.13}_{-0.15}$	$10.91^{+0.39}_{-0.92}$	$1.57^{+0.37}_{-0.31}$	$11.82^{+0.42}_{-0.82}$
M13	$1.48^{+0.21}_{-0.64}$	$11.04^{+1.00}_{-1.28}$	$0.901^{+0.28}_{-0.12}$	$12.21^{+0.18}_{-0.62}$
ω Cen	$1.43^{+0.26}_{-0.61}$	$11.18^{+1.14}_{-1.27}$	$0.994^{+0.51}_{-0.21}$	$12.09^{+0.27}_{-0.66}$
X7	$0.832^{+1.19}_{-0.051}$	$13.25^{+1.37}_{-3.50}$	$1.98^{+0.10}_{-0.36}$	$11.3^{+0.95}_{-1.03}$

Steiner, Lattimer, Brown, ApJ 2010

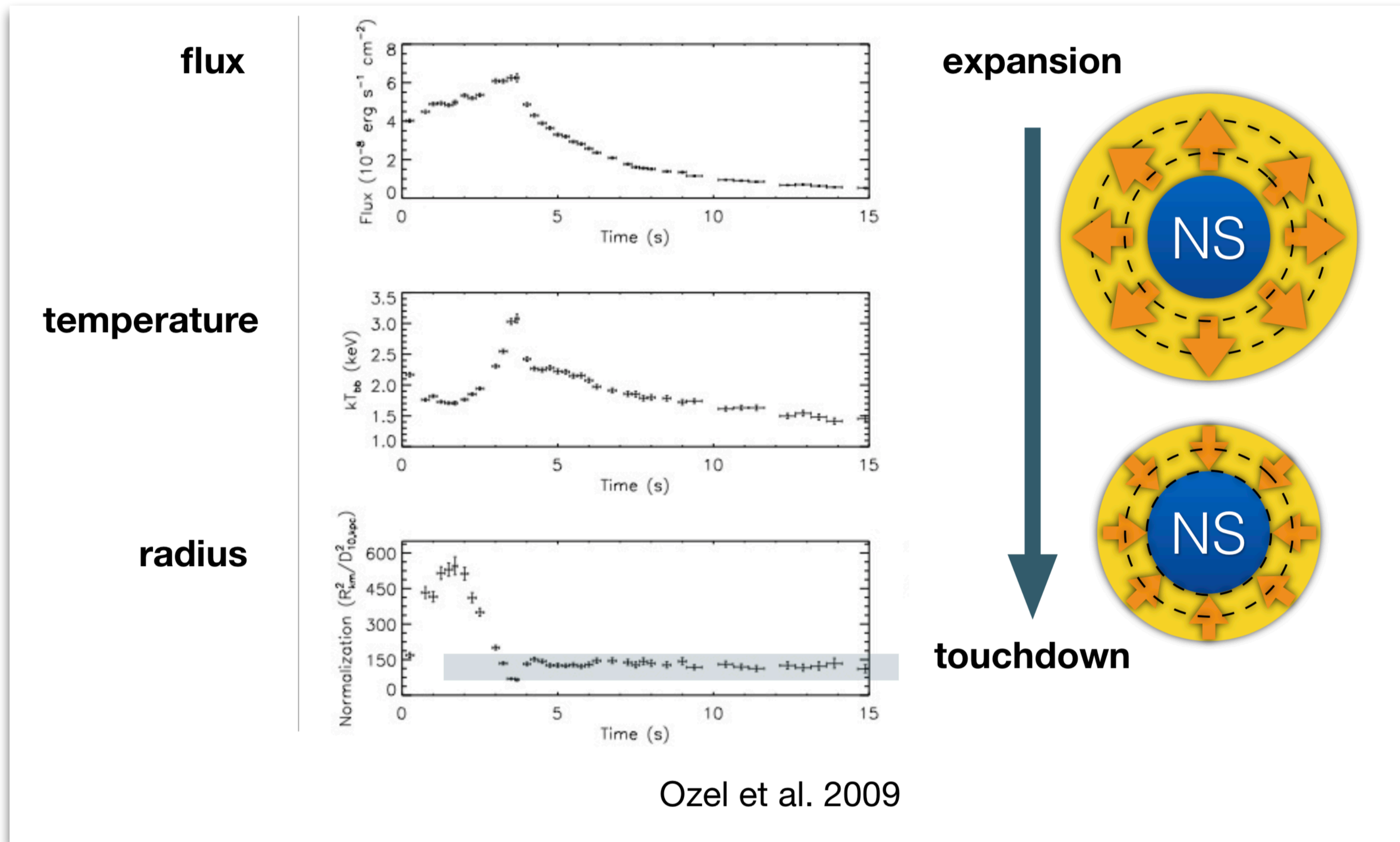
95% confidence limits by using MC sampling (for fixed NS mass)



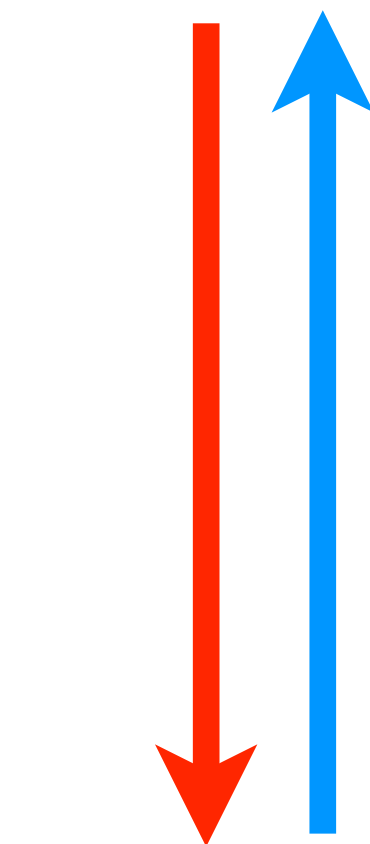
In this talk, I will focus on

- Low-Mass X-ray Binaries (LMXB) with Photospheric Radius Expansion (PRE)
- Simultaneous measurement of neutron star Mass & Radius

Photospheric Radius Expansion (PRE) XRB



Observations
 ($F_D, T; distance$)



(M, R)

Equations of state

LMXBs considered in our work

Table 1. Observational properties of six LMXBs that show PRE XRBs.

Source	App. angular area (km/10 kpc) ²	Touchdown flux (10 ⁻⁸ erg cm ⁻² s ⁻¹)	Spin freq. ^(a) (Hz)	Distance ^(a) (kpc)
4U 1820–30	89.9 ± 15.9	5.98 ± 0.66	...	7.6 ± 0.4 (4) 8.4 ± 0.6 (5–6)
SAX J1748.9–2021	89.7 ± 9.6	4.03 ± 0.54	410 (1)	8.2 ± 0.6 (4, 5, 7)
EXO 1745–248	117.8 ± 19.9	6.69 ± 0.74	...	6.3 ± 0.63 ^(b) (8–9)
KS 1731–260	96.0 ± 7.9	4.71 ± 0.52	524 (2)	7–9 ^(c) (10)
4U 1724–207	113.8 ± 15.4	5.29 ± 0.58	...	7.4 ± 0.5
4U 1608–52	314 ± 44.3	18.5 ± 2.0	620 (3)	4.0 ± 2.0, $D_{\text{cutoff}} > 3.9$ ^(d)

Our strategy

Observations
(F_D, T ; distance)

Steiner et al., ApJ 722, 33 (2010)

Ozel et al., ApJ 820, 28 (2016)

Method 1
Monte Carlo sampling
(M. Kim)

Method 2
Bayesian analysis (NS EOS is used)
(Y.-M. Kim)

(M, R)

Method 1: Monte Carlo sampling *(by M. Kim)*

Basic observations : flux, spectrum (blackbody temperature)

before corrections

Touch down flux $F_{\text{TD},\infty} = \frac{GMc}{\kappa D^2} \left(1 - \frac{2GM}{Rc^2}\right)^{1/2}$

Apparent angular area $A \equiv \frac{F_\infty}{\sigma T_{\text{bb},\infty}^4} = f_c^{-4} \frac{R^2}{D^2} \left(1 - \frac{2GM}{Rc^2}\right)^{-1}$

Opacity $\kappa = 0.2(1 + X) \text{ cm}^2 \text{ g}^{-1}$

X : hydrogen mass fraction in H-He plasma

Systematic treatments

- ***Color-correction factor***

- Change of the effective area due to the atmospheric effect

- ***Cooling tail method***

- Spectral evolution during the cooling phase due to the atmosphere of NS
(surface gravity & chemical composition)

- ***Chemical composition of the photosphere***

- H-He plasma

$$\kappa = 0.2(1 + X) \text{ cm}^2 \text{ g}^{-1}$$

X : hydrogen mass fraction in H-He plasma

Flux, Color temperature, Apparent area ($r_{\text{ph}} = R$)

$$F_{\text{TD},\infty} = \frac{GMc}{\kappa D^2} \left(1 - \frac{2GM}{Rc^2}\right)^{1/2} \left[1 + \left(\frac{kT_c}{38.8 \text{ keV}}\right)^{a_g} \left(1 - \frac{2GM}{Rc^2}\right)^{-a_g/2}\right],$$

where

$$a_g = 1.01 + 0.067 \log\left(\frac{g_{\text{eff}}}{10^{14} \text{ cm s}^{-2}}\right),$$

$$g_{\text{eff}} = \frac{GM}{R^2} \left(1 - \frac{2GM}{Rc^2}\right)^{-1/2},$$

$$T_c = f_c \left(\frac{g_{\text{eff}} c}{\sigma \kappa}\right)^{1/4} = f_c \left(\frac{GMc}{\sigma \kappa R^2}\right)^{1/4} \left(1 - \frac{2GM}{Rc^2}\right)^{-1/8}.$$

$$A = f_c^{-4} \frac{R^2}{D^2} \left(1 - \frac{2GM}{Rc^2}\right)^{-1} \left\{1 + \left[\left(0.108 - 0.096 \frac{M}{M_\odot}\right) + \left(-0.061 + 0.114 \frac{M}{M_\odot}\right) \frac{R}{10 \text{ km}} - 0.128 \left(\frac{R}{10 \text{ km}}\right)^2\right] \left(\frac{f_{\text{NS}}}{1000 \text{ Hz}}\right)^2\right\}^2.$$

$$r_{\text{ph}} \neq R$$

$$F_{\text{TD},\infty} = \frac{GMc}{\kappa D^2} \left(1 - \frac{2GM}{r_{\text{ph}}c^2}\right)^{1/2} \left[1 + \left(\frac{kT_c}{38.8 \text{ keV}}\right)^{a_g} \left(1 - \frac{2GM}{r_{\text{ph}}c^2}\right)^{-a_g/2}\right],$$

where

$$a_g = 1.01 + 0.067 \log \left(\frac{g_{\text{eff}}}{10^{14} \text{ cm s}^{-2}}\right),$$

$$g_{\text{eff}} = \frac{GM}{r_{\text{ph}}^2} \left(1 - \frac{2GM}{r_{\text{ph}}c^2}\right)^{-1/2},$$

$$T_c = f_c \left(\frac{g_{\text{eff}}c}{\sigma\kappa}\right)^{1/4} = f_c \left(\frac{GMc}{\sigma\kappa r_{\text{ph}}^2}\right)^{1/4} \left(1 - \frac{2GM}{r_{\text{ph}}c^2}\right)^{-1/8}.$$

Modifications

touchdown radius parameter

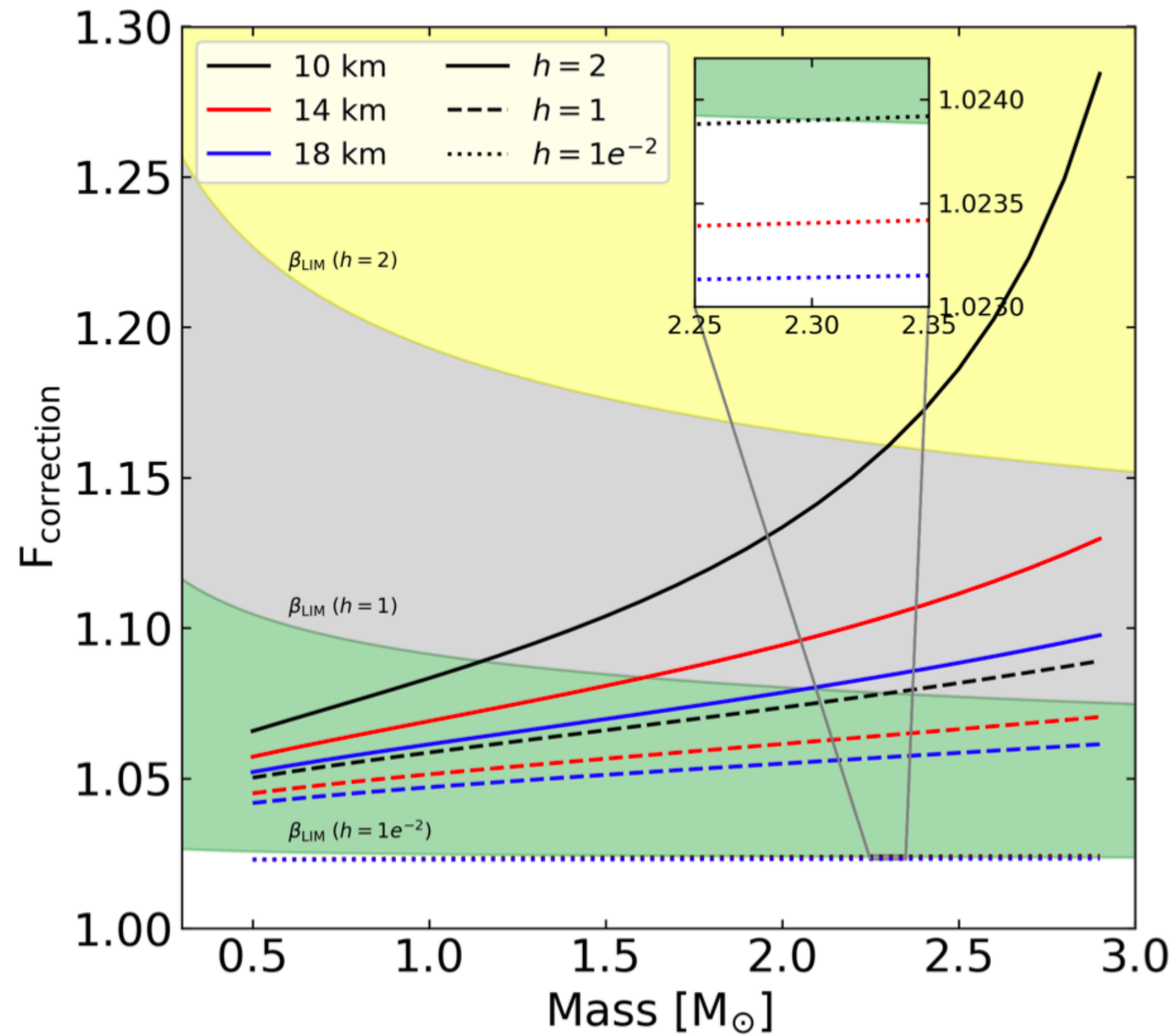
$$h = \frac{2R_{\text{NS}}}{r_{\text{ph}}}$$

causality limit

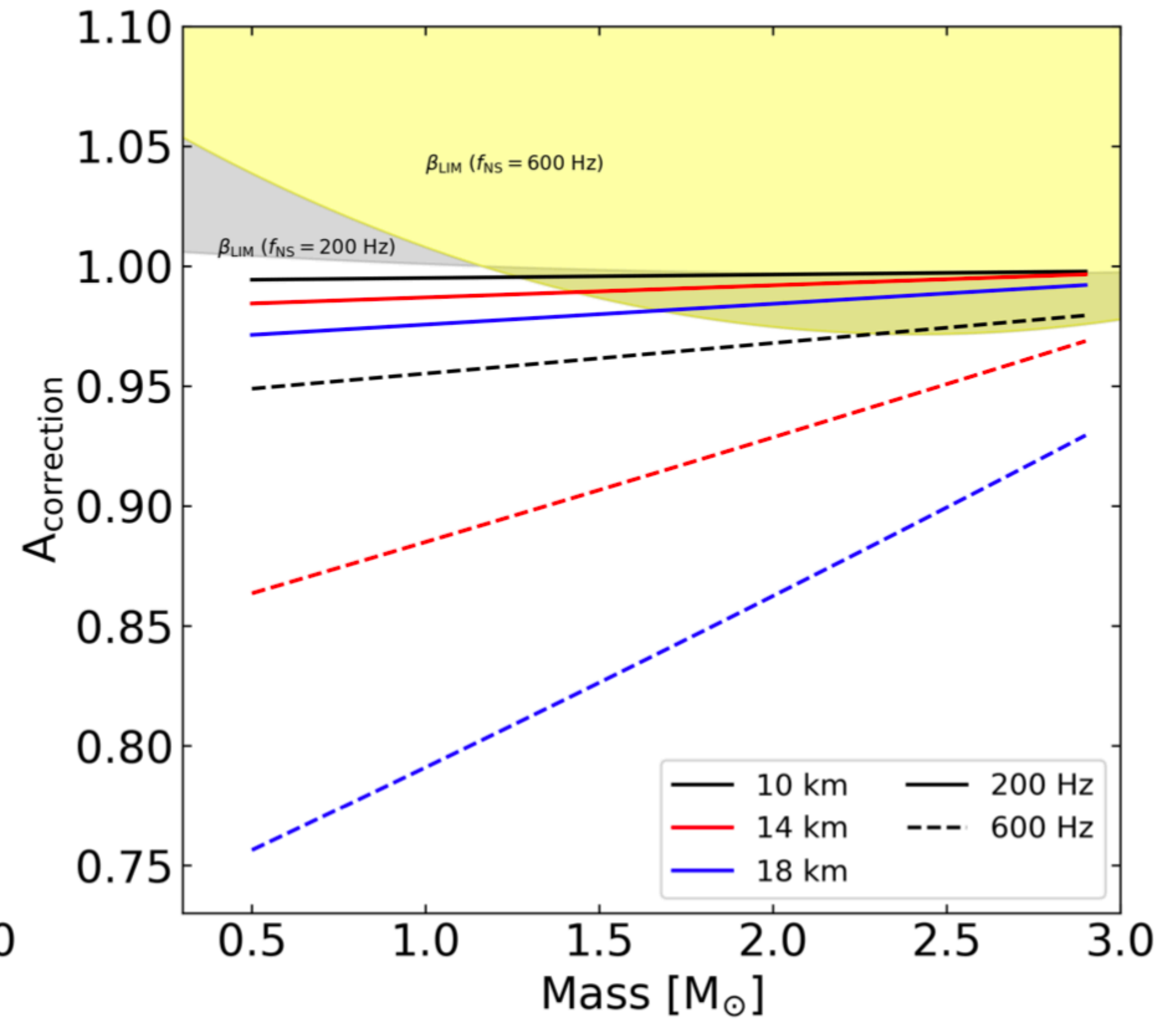
$$\beta = \frac{M_{\text{NS}}}{R_{\text{NS}}} < \frac{1}{2.94}$$

NS spin frequency

$$f_{\text{NS}}$$

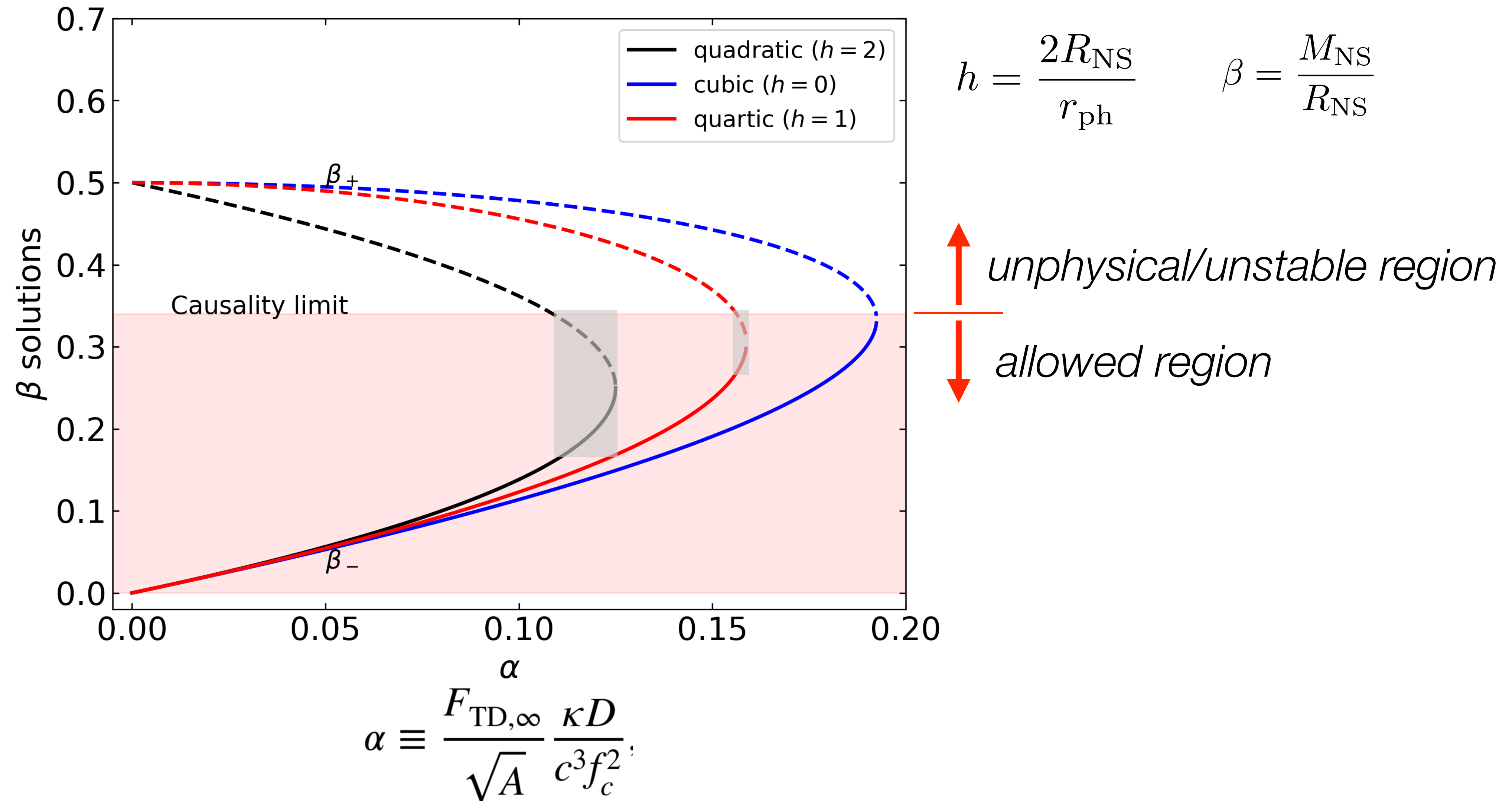


Touchdown Flux (ratio)

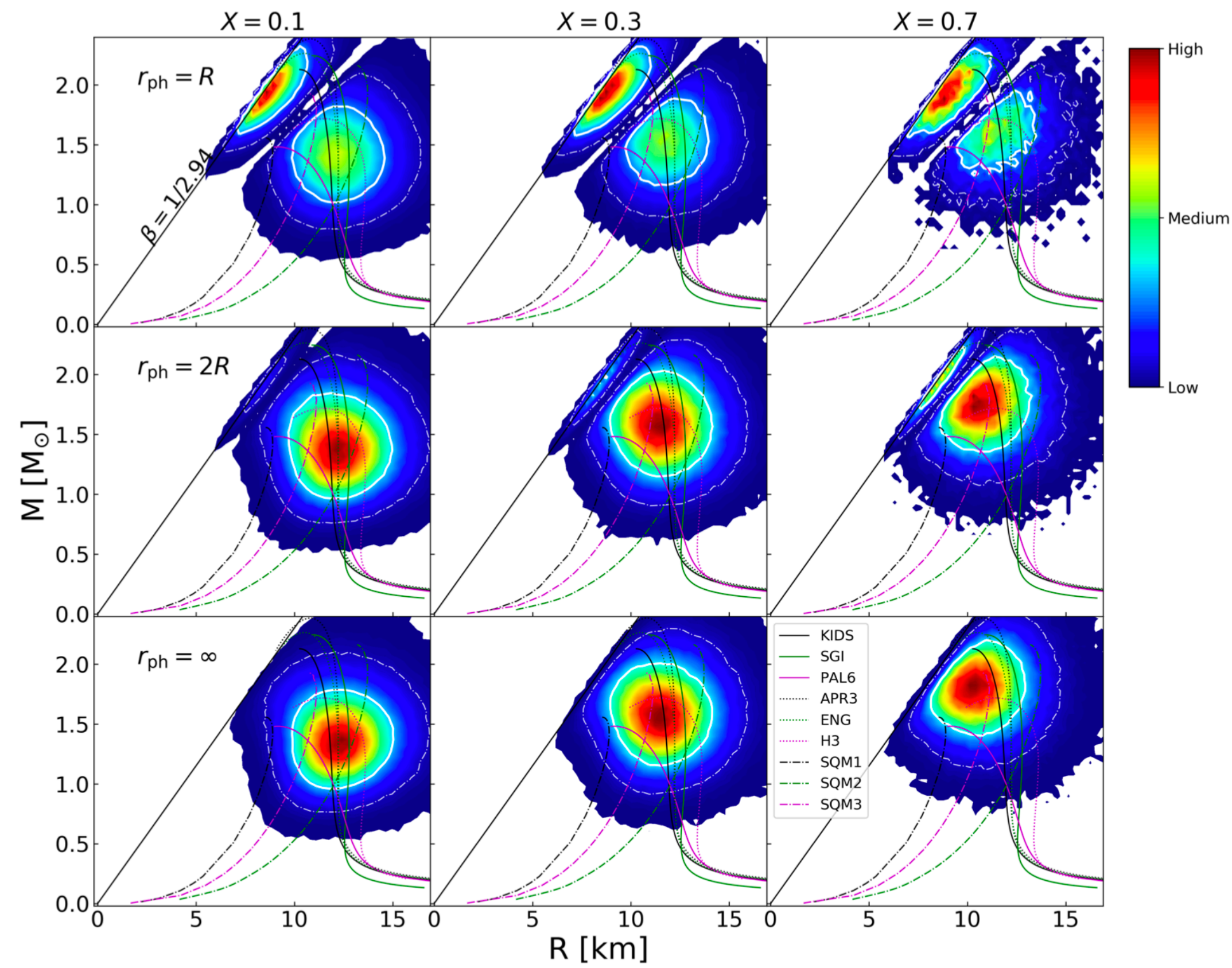


Apparent angular area (ratio)

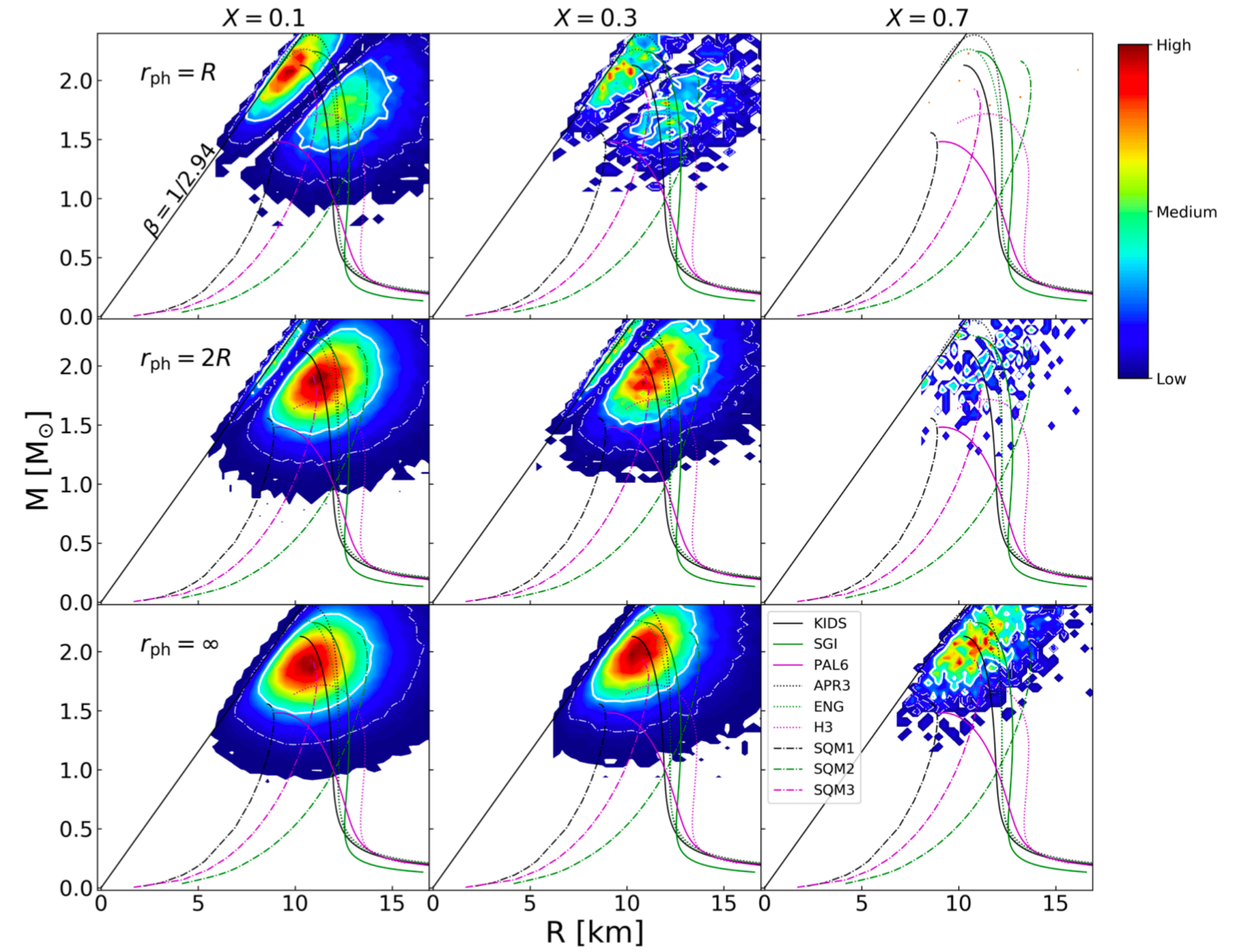
Double solutions are allowed in MC sampling



X: hydrogen mass fraction



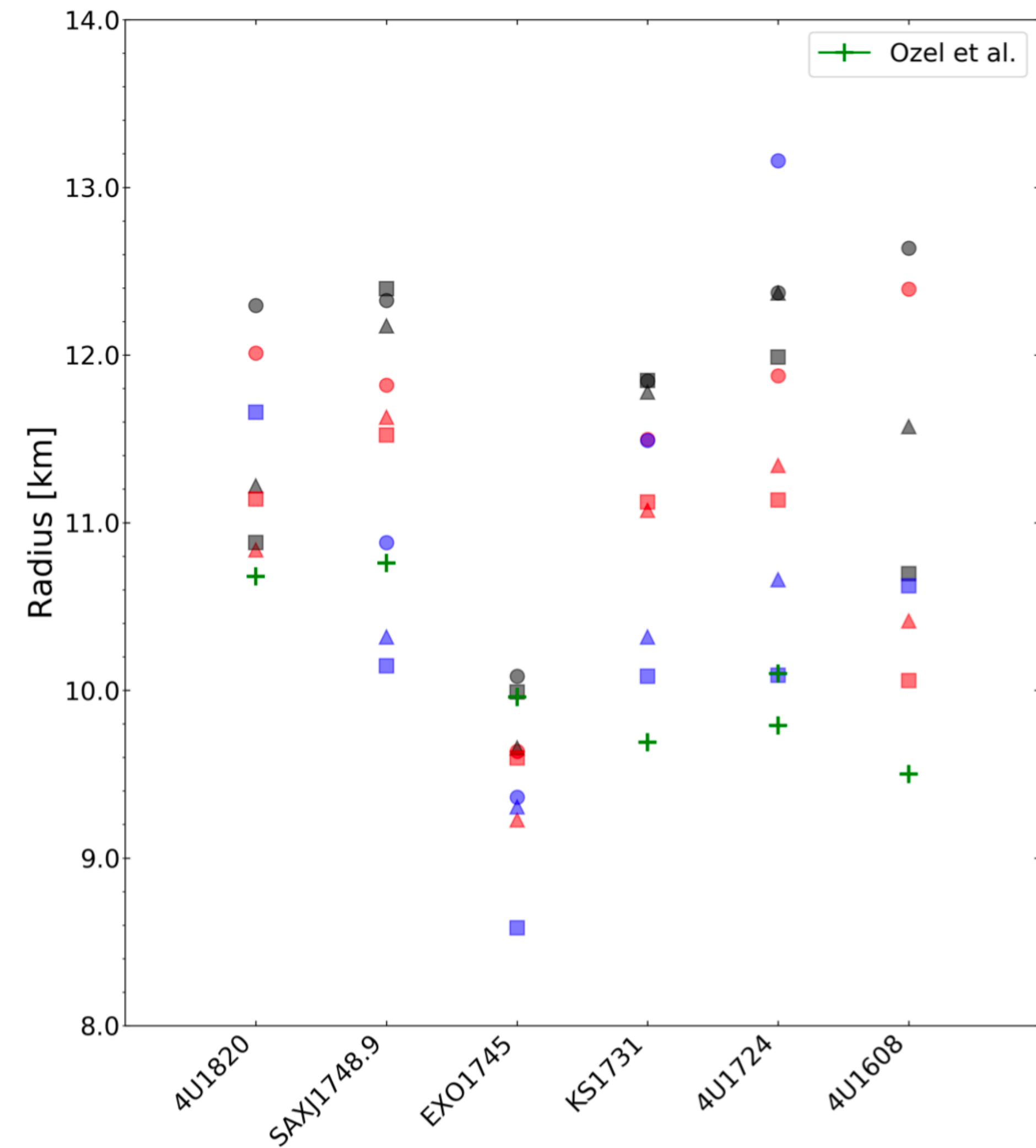
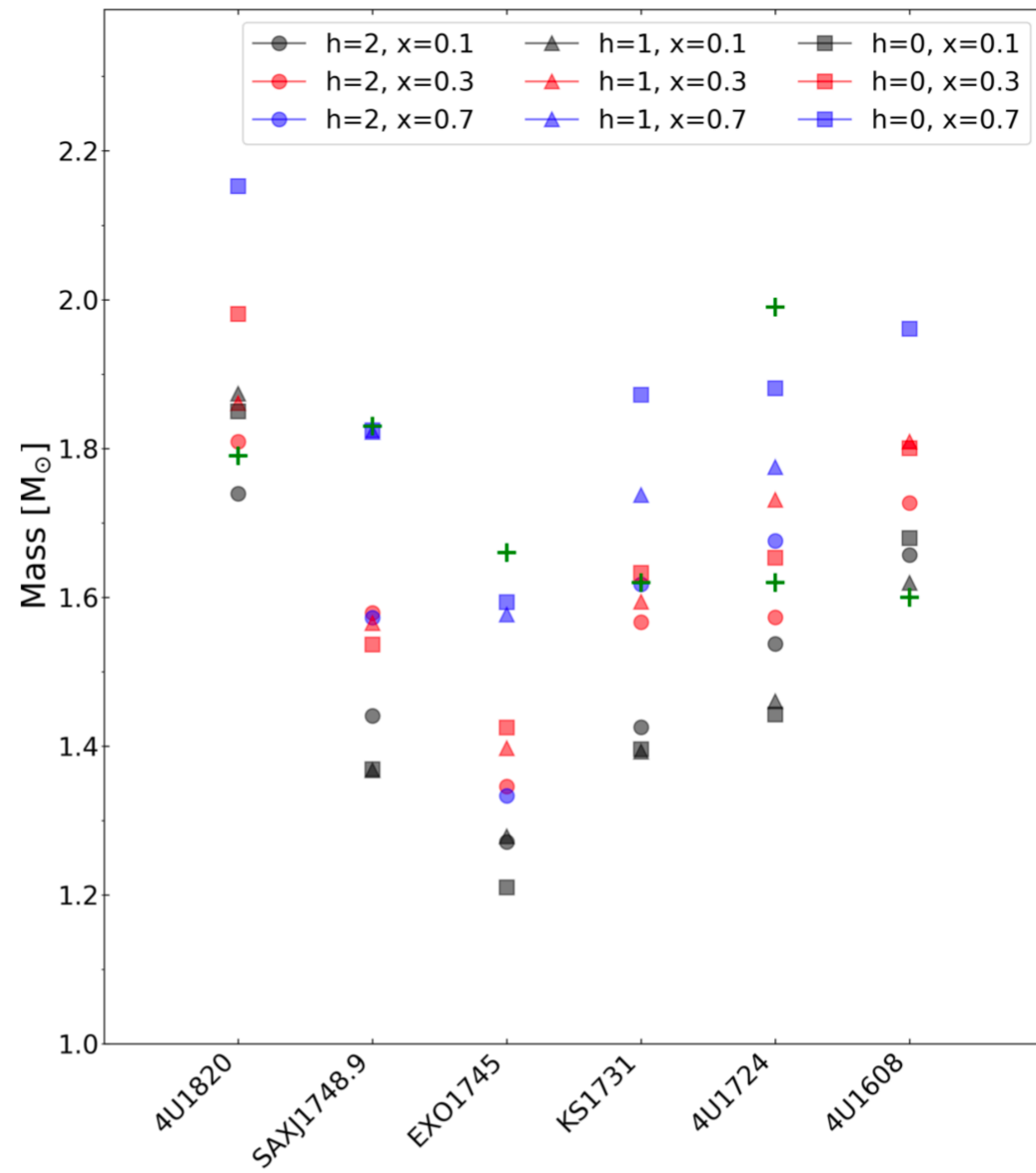
SAX J1748.9-2021



4U 1820-30

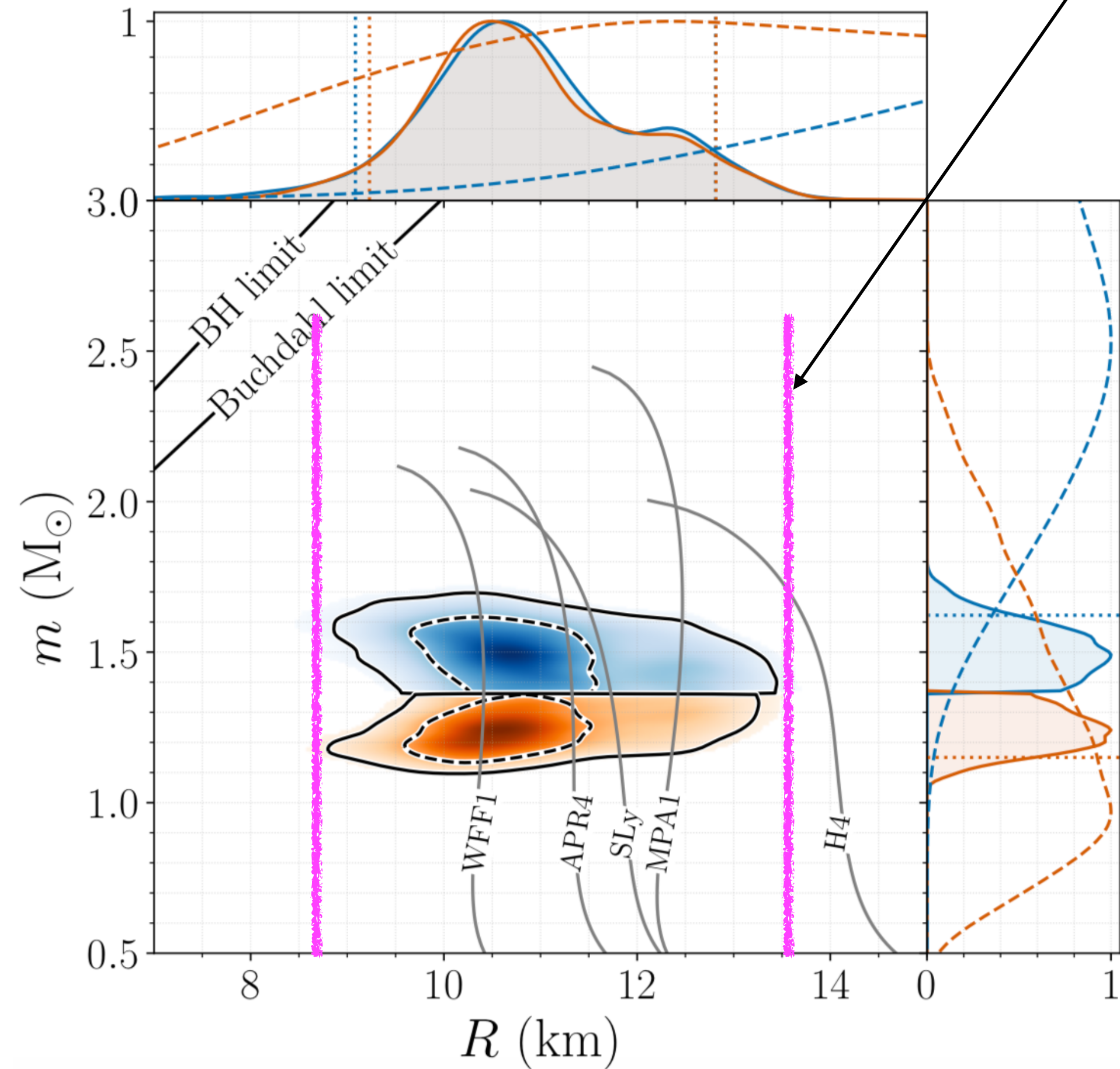
Most probable values of M & R

M. Kim, Y.-M. Kim et al. (A&A 2021)

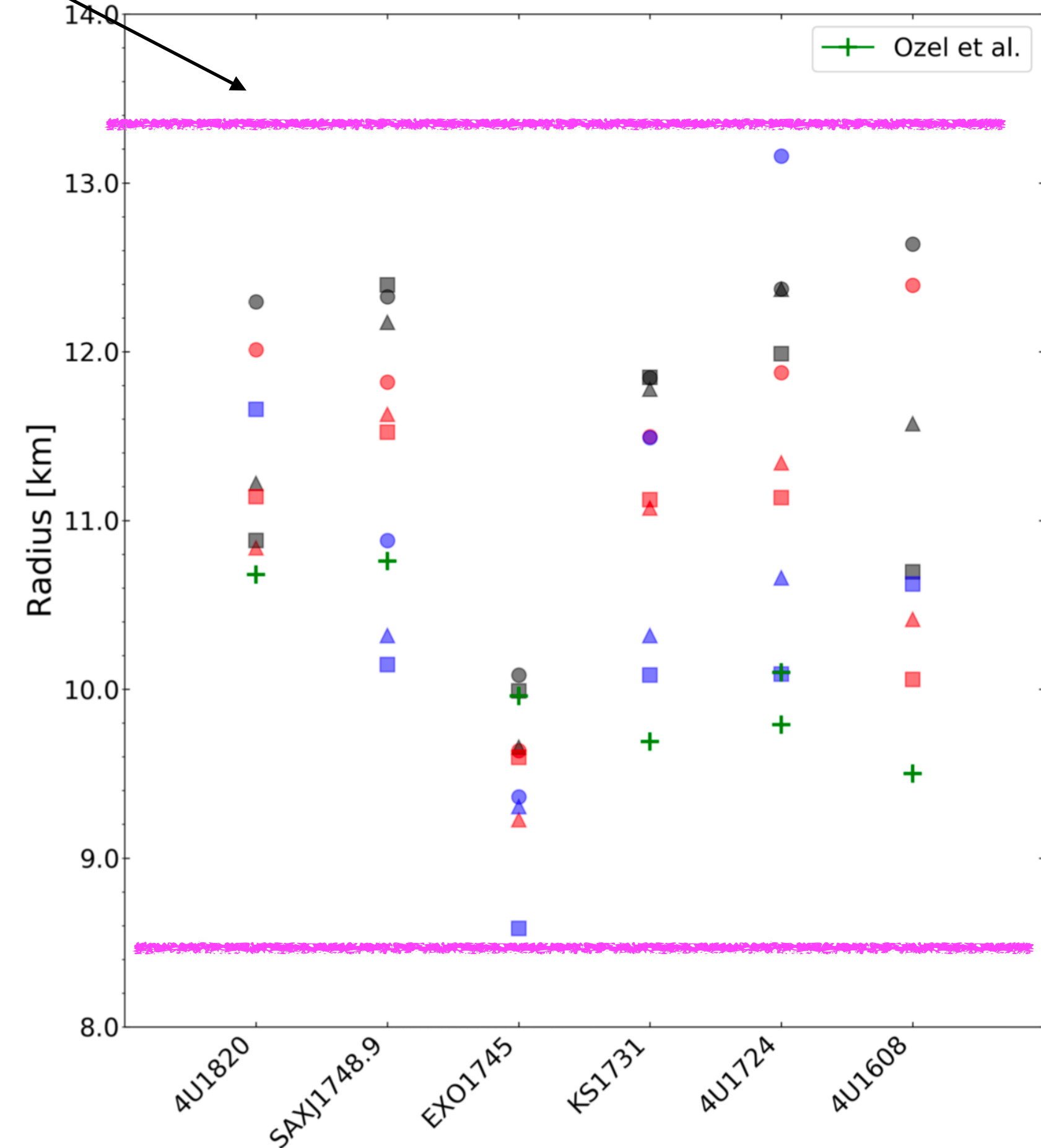


Most probable M,R

Consistent



Abbott et al. (LSC and Virgo), PRL 121.161101



M. Kim, Y.-M. Kim et al. (A&A 2021)

Method 2: Bayesian analysis *(by Y.-M. Kim)*

$$P(\boldsymbol{\theta}|\text{data}) = \frac{P(\text{data}|\boldsymbol{\theta})P(\boldsymbol{\theta})}{P(\text{data})}$$

Posterior probability distribution

$$\boldsymbol{\theta} = \{R, M, D, f_{\text{NS}}, f_{\text{c}}, X, h\}$$

Parameter set

$$P(\text{data}|\boldsymbol{\theta})$$

Likelihood

$$P(\boldsymbol{\theta})$$

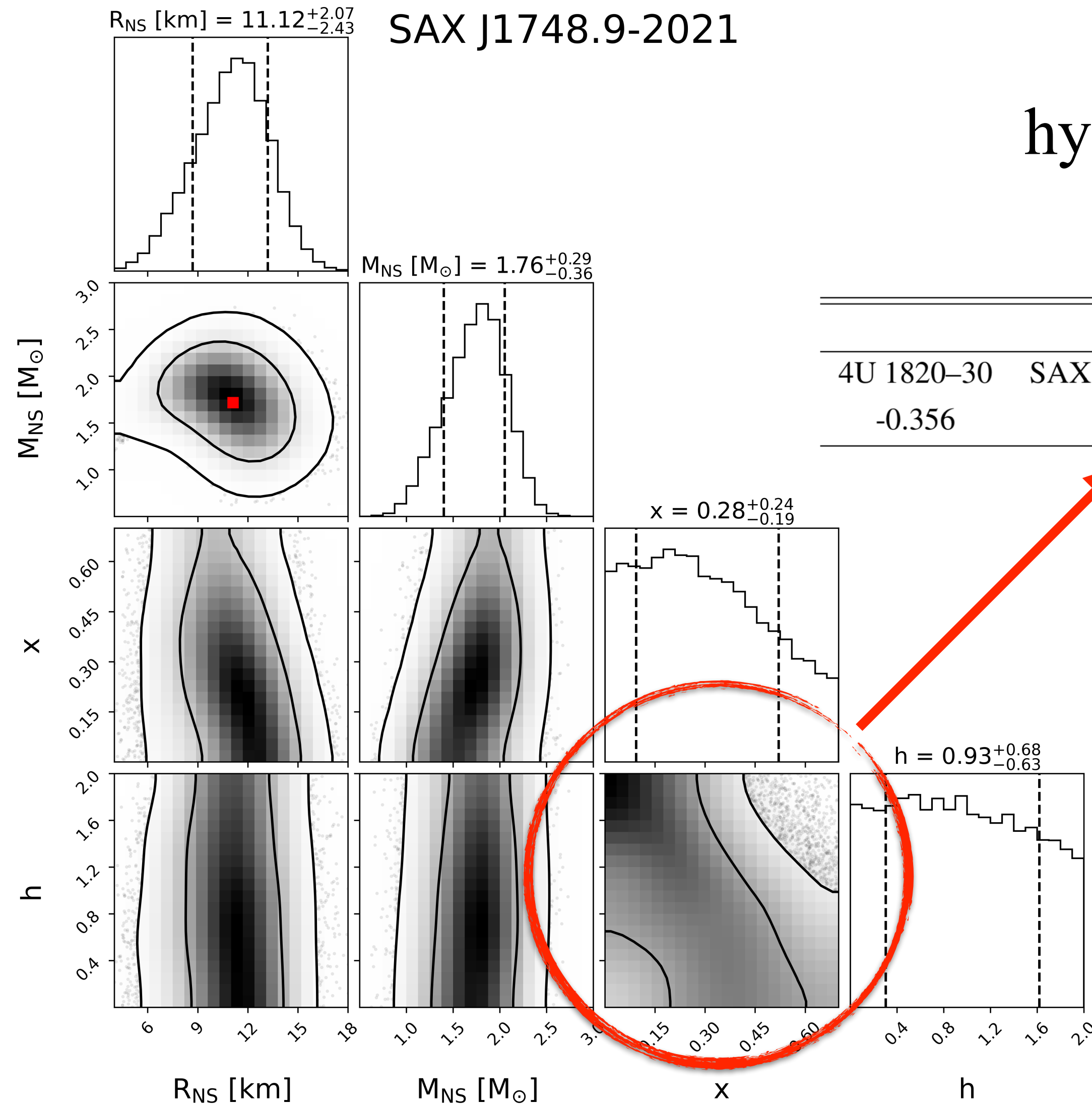
Prior of the parameter set of the model

$$P(\boldsymbol{\theta}) = P(R)P(M)P(D)P(f_{\text{NS}})P(f_{\text{c}})P(X)P(h)$$

(flat distribution for unknown quantities without using EOS)

Mass-Radius estimation by Bayesian.

$$h = \frac{2R_{\text{NS}}}{r_{\text{ph}}}$$



Correlation of hydrogen mass fraction, x Photosphere size, h

Pearson correlation coefficient (R)					
4U 1820-30	SAX J1748.9-2021	EXO 1745-248	KS 1731-260	4U 1724-207	4U 1608-52
-0.356	-0.622	-0.526	-0.539	-0.631	-0.529

M. Kim, Y.-M. Kim et al. (A&A 2021)

Discussions on LMXBs

- LMXBs are good laboratories for NS physics
 - Photosphere is likely to be **H-poor** regardless of the energy generation mechanism below.
 - Touchdown is likely to occur **away** from the neutron star surface.
 - Bounds of NS radius is consistent with the results of LIGO/Virgo (based on tidal deformability of GW170817).
- Future observations of LMXBs will be able to give more constraints on NS masses & radii, and check the possibilities of Quark Stars.
- Effects of accretion disk in LMXBs are in progress.



Symmetry

yangzhou@2023.09.22